

# Dielectric properties of $\text{CaCu}_3\text{Ti}_4\text{O}_{12}$ based multiphased ceramics

**S. Guillemet-Fritsch, T. Lebey, M. Boulos and B. Durand**

Centre InterUniversitaire de Recherche et d'Ingénierie des Matériaux (CIRIMAT/LCMIE),  
Université Paul Sabatier, Bât. 2R1, 118, Route de Narbonne, 31062 Toulouse Cedex 04,  
France

Laboratoire de Génie Electrique de Toulouse (LGET), Université Paul Sabatier, Bât. 3R3,  
118, Route de Narbonne, 31062 Toulouse Cedex 04, France

## Abstract

A “soft chemistry” method, the coprecipitation, has been used to synthesize the perovskite  $\text{CaCu}_3\text{Ti}_4\text{O}_{12}$  (CCT). Three main types of materials were obtained for both powders and sintered ceramics: a monophased consisting of the pure CCT phase, a biphased ( $\text{CCT} + \text{CaTiO}_3$ ), and a three-phased ( $\text{CCT} + \text{CaTiO}_3 + \text{copper oxide (CuO or Cu}_2\text{O)}$ ). These ceramics, sintered at low temperature, 1050 °C, present original dielectric properties. The relative permittivity determined in the temperature range ( $-150 < T < 250$  °C) is significantly higher than the one reported in the literature. Internal barrier layer capacitor is the probable mechanism to explain the particular behaviour. Moreover, the presence of a copper oxide phase beside the perovskite CCT plays an important role for enhancing the dielectric properties.

**Keywords:** Powders-chemical preparation; Sintering; Dielectric properties;  $\text{CaCu}_3\text{Ti}_4\text{O}_{12}$ ; Capacitors

1. Introduction
2. Experimental

- 2.1. Sample preparation
- 2.2. Characterization
- 3. Results
  - 3.1. Powders
  - 3.2. Ceramics
- 4. Discussion
- 5. Conclusion
- Acknowledgements
- References

## **1. Introduction**

Many research have been done recently on the synthesis and characterization of the cubic perovskite  $\text{CaCu}_3\text{Ti}_4\text{O}_{12}$ , or  $\text{Ca}_{0.25}\text{Cu}_{0.75}\text{TiO}_3$  ceramic (commonly called CCT), because of its unusual electrical properties. Subramanian et al.<sup>1</sup> have first reported the high dielectric constant at 1 kHz in  $\text{ACu}_3\text{Ti}_4\text{O}_{12}$  and  $\text{ACu}_3\text{Ti}_3\text{FeO}_{12}$  phases (A = trivalent rare earth or Bi). Permittivity values ( $\epsilon'$ ) higher than 10,000 have been reported for ceramics<sup>1 and 2</sup> and for single crystals.<sup>3</sup>

The real part of the permittivity has been even increased from 10,000 to 300,000, as a result of grain growth.<sup>4</sup> Studies of  $\text{CaCu}_3\text{Ti}_4\text{O}_{12}$  thin films prepared by pulsed laser deposition confirm that large mean grain size may be responsible for the high dielectric constant.<sup>5</sup> Moreover, the high dielectric constant does not depend on the temperature, which makes it even more attractive for technological applications, even if the dielectric losses, which are in most cases very high, have also to be taken into account.

The crystal structure of CCT, determined from powder neutron diffraction method<sup>6 and 7</sup> is well described in the space group  $Im\bar{3}$ . The stabilization of the observed structure is attributed to the strong preference of Cu for the square planar geometry. No phase transition has been detected between 25 and 1000 °C, neither using powder diffraction<sup>7</sup> nor by Raman spectroscopy studies.<sup>8</sup>

Though different hypotheses have been given to explain the high permittivity value, its origin is not fully understood. Subramanian et al.<sup>1 and 2</sup> suggested that the polarizability and the dielectric constant are enhanced by the tension on the Ti—O bonds, but that the transition to the ferroelectric state is frustrated by the  $\text{TiO}_6$  octahedra tilt structure that accommodates the square planar coordination of  $\text{Cu}^{2+}$ . According to the same authors, the dielectric constant of the CCT ceramic is also enhanced by its microstructure and is sensitive to the Cu/Ca ratio. A

characteristic gap energy of 28 meV was calculated for the relaxational mode.<sup>2</sup> In a more recent work, the same authors<sup>9</sup> indicated that the numerous twins observed in CCT single crystals may influence the dielectric properties and that the very high dielectric constant of  $\text{CaCu}_3\text{Ti}_4\text{O}_{12}$  might be an extrinsic property. Cohen et al.<sup>10</sup> also suggested that the large dielectric constant observed in CCT monocrystals probably arisen from spatial inhomogeneities of local dielectric response, like twins, Ca ordering and antiphase boundaries. Hassini et al.,<sup>11</sup> using infrared spectroscopy, indicated that the high permittivity value is not related to phonons but rather to a relaxational motion of Debye-type with a characteristic relaxation time expected in the gigahertz range. Sinclair et al.<sup>4</sup> believed, according to impedance spectroscopy studies, that the high permittivity is associated to internal barrier layer capacitor and not to an intrinsic feature of the bulk crystal structure. They demonstrated that  $\text{CaCu}_3\text{Ti}_4\text{O}_{12}$  ceramics are electrically heterogeneous and consist of semiconducting grains with insulating grain boundaries. They also showed the influence on the effective permittivity of the ceramic grain size, obtained from various dwell time at the sintering temperature.<sup>12</sup> The “giant” effective permittivity value for the ceramics sintered for 24 h has been associated to the presence of, either thin reoxidized grain boundary regions on the outer surface of the large semiconducting grains, or to a secondary phase at the grain boundaries which has not been detected by SEM. Homes et al.,<sup>13</sup> using infrared measurements on  $\text{CaCu}_3\text{Ti}_4\text{O}_{12}$  and  $\text{CdCu}_3\text{Ti}_4\text{O}_{12}$ , agree with the internal barrier layer capacitance effect, as well as Lunkenheimer et al.,<sup>14</sup> that explain the colossal effect by Maxwell–Wagner-type contributions of depletion layers at the interface between sample and contacts or at grain boundaries. Optical conductivity measurements on CCT single crystals have provided more information about the physics explaining the giant dielectric effect in this material.<sup>3</sup> The discrepancy, noticed between low dielectric constant (80) at infrared frequencies and high constant ( $10^5$ ) at lower radio frequencies, indicates a strong absorption due to dipole relaxation. So, in the last few years, several authors considered that the exceptional dielectric properties of CCT are due to opposite electrical properties of the bulk and internal boundaries regions (one is insulating and the other conducting).

Most of the papers reported in the literature mentioned that the CCT materials studied were single phased (CCT). Only Subramanian et al.<sup>2</sup> indicated the presence of a minute impurity of CuO detected by X-ray diffraction analysis. Kobayashi et al.<sup>15</sup> showed a drop of  $\epsilon'$  for a factor  $10^2$  when introducing impurities (manganese) and explained it by a dipole moment causing fluctuating ferroelectric domains in  $\text{CaCu}_3\text{Ti}_4\text{O}_{12}$ .

Most of the CCT samples were obtained by solid/solid reactions. Nanocrystalline CCT powders were also prepared by mechanical alloying.<sup>16</sup> Only few “soft chemistry” methods were used to prepare CCT. The polymeric citrate precursor route was mentioned.<sup>17</sup> The powder grains prepared from this method are smaller than the ones obtained by solid/solid reaction. The dielectric constant is also higher in the first case, but largely lower than the  $10^4$  reported by Subramanian.<sup>1</sup> Hassini et al.<sup>11</sup> synthesized both  $\text{CaCu}_3\text{Ti}_4\text{O}_{12}$  and  $\text{CaTiO}_3$  by an organic gel-assisted citrate process, described in.<sup>18</sup>

In this paper, we present new results concerning the elaboration of CCT powders by the coprecipitation method. The elaboration of the corresponding ceramics and their physico-chemical characterization are then described. Finally, the influence of the structure (presence of additional phases) and the microstructure (grain size) on the dielectric properties of the ceramics is shown.

## **2. Experimental**

### **2.1. Sample preparation**

The CCT powders were prepared using one of a soft chemistry technique, i.e. the coprecipitation of oxalate precursors. The starting materials were:  $\text{TiCl}_3$  (Prolabo,  $d = 1.20$ , %min = 15),  $\text{CaCl}_2$  (Prolabo, %min = 96) and  $\text{CuCl}_2 \cdot 2\text{H}_2\text{O}$  (Prolabo, %min = 99). They were dissolved in water in various proportions and the coprecipitation was performed by addition of a solution of oxalic acid dissolved in ethanol.  $\text{TiCl}_3$  was chosen because it was easier to handle than  $\text{TiCl}_4$ . The full oxidation of  $\text{Ti}^{3+}$  in  $\text{Ti}^{4+}$  in the solution was ensured by air bubbling during the reaction. It was evidenced by the visual observation of the color variation from white to clear blue. The volume of water was taken much lower than the one of ethanol, in order to decrease the dielectric constant of the precipitation media. Since the nucleation of the particles is favoured compared to the growth, smaller particles, homogeneous in size and composition, are likely to be obtained.<sup>19</sup> The solution was aged for a couple of hours, and the precipitate obtained was centrifuged. The precursors were then pyrolyzed in air at  $900\text{ }^\circ\text{C}$  for 10 h to obtain the oxides. These powders were mixed with an organic binder, then uniaxially pressed into disk (diameter: 6 mm and thickness: 1.5 mm) under 250 MPa pressure. Green ceramics were sintered in static air at  $1050\text{ }^\circ\text{C}$  for 24 h.

### **2.2. Characterization**

The accurate chemical composition of the oxide powder was determined by analyzing the Ni and Mn cations, using an induced coupled plasma spectroscopy (ICP AES Thermo-Optec ARL3580). Three trials were performed for each sample and the average value was calculated. The oxide powder morphology was observed with a Scanning Electron Microscope (JEOL JSM-6400). In some cases, backscattered electrons were used to obtain an image in chemical contrast. The specific surface area was determined using a Micrometrics accuserb 2100 E. The phase composition was determined by X-ray diffraction analysis: the data were collected with a SEIFERT XRD-3003-TT diffractometer using the Cu K $\alpha$  radiation ( $\lambda = 0.15418$  nm).

The electrical characterization consists in measuring the effective permittivity  $\epsilon^*$  using a Hewlett Packard HP 4284A precision LCR meter. The domains explored were 20 Hz to 1 MHz for the frequency, ambient to 160 °C for the temperature. A sinusoidal voltage of magnitude 1 VAC was applied. In some particular cases and thanks to DEA system, the permittivity is measured between 0.1 Hz and 100 kHz and from -120 to 220 °C. It has been checked that this change in the experimental set up has no impact on the values obtained.

## **3. Results**

### **3.1. Powders**

The chemical composition, the phase composition, the specific surface area and the crystallite size of the different powders prepared by pyrolysis of the oxalate precursors at 900 °C for 10 h are reported in [Table 1](#). The X-ray diffraction patterns are given in [Fig. 1](#). With the different amount of calcium, copper and titanium analysed in the oxide powder, three different kinds of materials were obtained: almost pure cubic CaCu<sub>3</sub>Ti<sub>4</sub>O<sub>12</sub> (JCPDS 75-2188) (a minute impurity of CaTiO<sub>3</sub> is observed), named CCT-A; CaCu<sub>3</sub>Ti<sub>4</sub>O<sub>12</sub> and a significant amount of the CaTiO<sub>3</sub> phase (JCPDS 46-2400) (CCT-B), and a mixture of three phases: CaCu<sub>3</sub>Ti<sub>4</sub>O<sub>12</sub>, CaTiO<sub>3</sub> and copper oxide, CuO (JCPDS 80-1917) (CCT-C series). In the case of polyphased material, the amount of the second or third phase (CaTiO<sub>3</sub> and CuO) was estimated from the ratio of the relative maximal peak intensity of the two phases CCT/CaTiO<sub>3</sub> and CCT/CuO ([Table 1](#)). The influence of the initial chemical composition of the oxide powder (Ca, Cu, Ti content) on the different phases formation is obvious. As expected, the pure CaCu<sub>3</sub>Ti<sub>4</sub>O<sub>12</sub> phase is obtained only when the ratio of calcium, copper and titanium are close to the stoichiometric ones. The CaTiO<sub>3</sub> phase appears if an excess of titanium is present,

and at the same time when the copper content slightly decreases. We suggest that it is the excess of titanium that leads to the precipitation of  $\text{CaTiO}_3$ , even if there is no excess of calcium. Since both Ca and Ti form a second phase, Cu is then in excess, with respect with the stoichiometry of  $\text{CaCu}_3\text{Ti}_4\text{O}_{12}$ . Hence the precipitation of the copper oxide CuO is observed, beside the CCT and  $\text{CaTiO}_3$  phases, when the titanium content is lower than 4.00 (CCT-C series), and as the copper content varies in the range 2.68–3.24. So we can suggest that the Ti content mostly controls the phase composition (single or multiphased material) of the CCT powder. There is no data on the phase diagram of the Ca/Cu/Ti/O system in the literature. The present study points out that the cubic perovskite  $\text{CaCu}_3\text{Ti}_4\text{O}_{12}$  is a defined compound.

Table 1.

Chemical analysis, phase composition, specific surface area and crystallite size of the  $\text{Ca}_x\text{Cu}_y\text{Ti}_z\text{O}_{12}$  oxide powders obtained at 900 °C in air

Reference	Chemical analysis			Phase composition	Intensity ratio <sup>a</sup> CCT/CaTiO <sub>3</sub>	Intensity ratio CCT/CuO	$S_w$ (m <sup>2</sup> /g) <sup>b</sup>	$d_{\text{BET}}$ (nm) <sup>c</sup>
	x Ca	y Cu	z Ti					
CCT-A	1.2 4	2.7 6	4.0 0	CCT <sup>d</sup> (+ traces CaTiO <sub>3</sub> )	21	–	3.0	400
CCT-B	1.8 8	2.1 2	4.0 0	CCT+CaTiO <sub>3</sub>	5	–	6.8	200
CCT-C1	1.4 0	2.8 8	3.7 2	CCT+ CaTiO <sub>3</sub> +Cu O	5	6	2.0	600
CCT-C2	1.6 4	2.6 8	3.6 8	CCT+ CaTiO <sub>3</sub> +Cu O	10	11	2.6	450
CCT-C3	1.1 2	3.2 4	3.6 4	CCT+ CaTiO <sub>3</sub> +Cu O	15	10	1.6	740

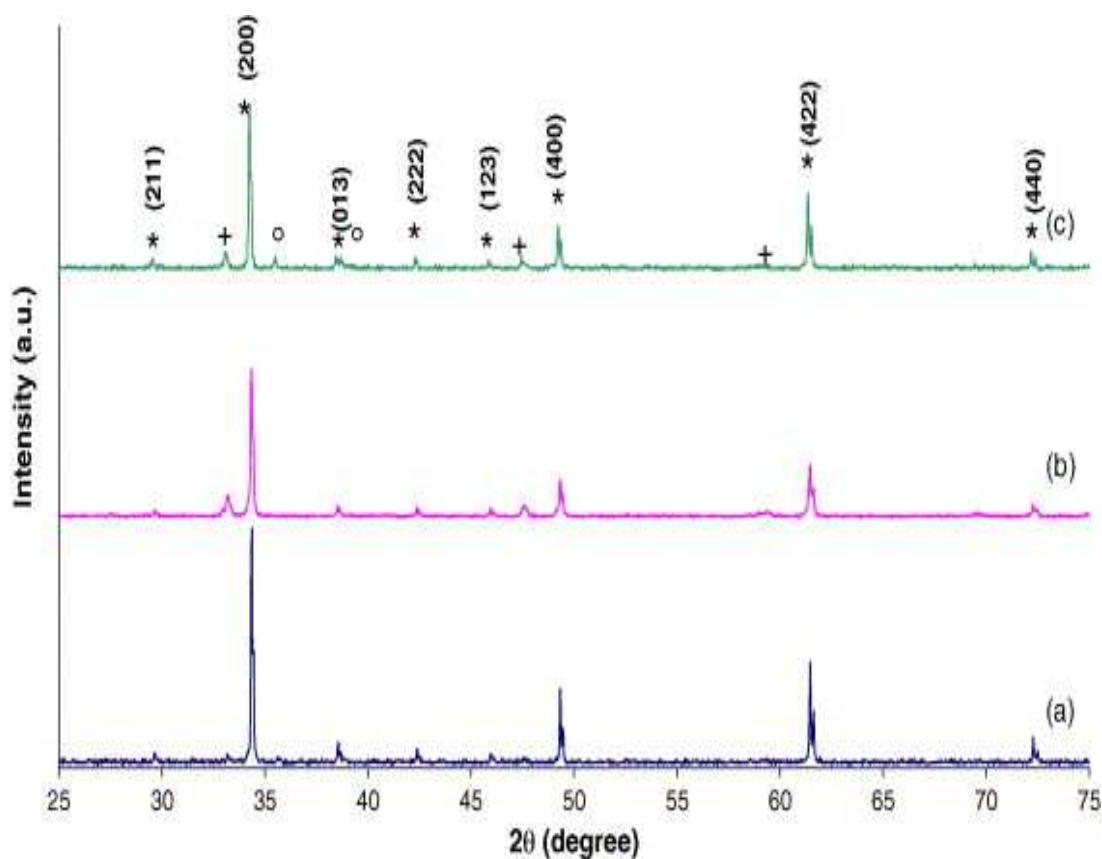
<sup>a</sup> Estimated from the relative ratio of the maximal peak intensity of the two phases.

<sup>b</sup> Determined from BET measurements.

<sup>c</sup> Calculated from specific surface area data.

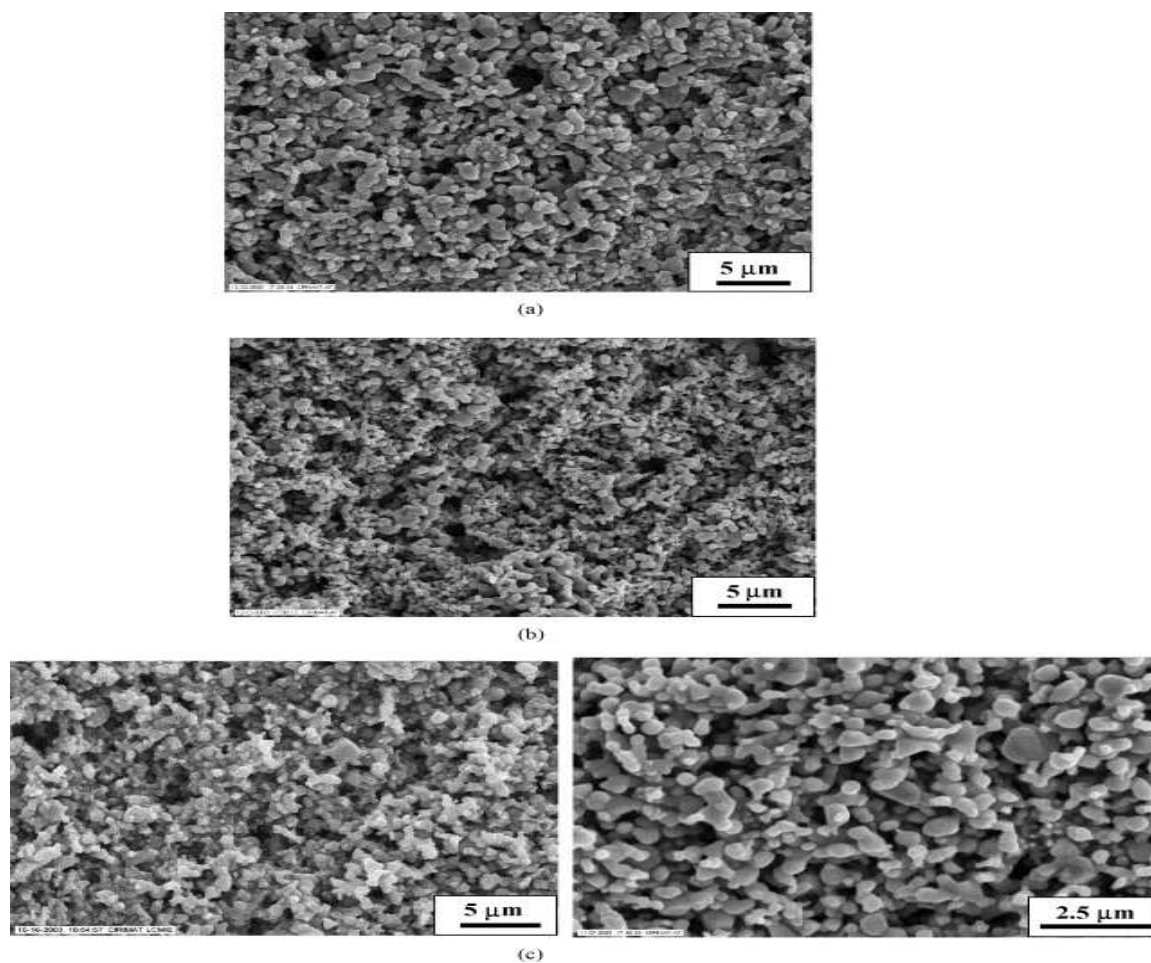
<sup>d</sup> CCT means  $\text{CaCu}_3\text{Ti}_4\text{O}_{12}$ .

Fig. 1. X-ray diffraction pattern of CCT-based powders calcined at 900 °C for 10 h. CCT-A: monophased  $\text{Ca}_{0.25}\text{Cu}_{0.75}\text{TiO}_3$  (\*) (a), CCT-B:  $\text{Ca}_{0.25}\text{Cu}_{0.75}\text{TiO}_3$  (\*) and  $\text{CaTiO}_3$  (+) (b) and CCT-C1:  $\text{Ca}_{0.25}\text{Cu}_{0.75}\text{TiO}_3$  (\*),  $\text{CaTiO}_3$  (+) and  $\text{CuO}$  (o) (c).



The specific surface area and the crystallite size deduced from our data do not vary much in the whole studied composition range (Table 1). Only the CCT-B powder seems to have smaller grains, for unclear reasons. So the presence of  $\text{CaTiO}_3$  and  $\text{CuO}$  beside the CCT phase does not influence the powder reactivity. SEM observations of the calcined powders (Fig. 2) indicate that the grains are homogeneous in shape and size, approximately ranging from 0.5 to 1.5  $\mu\text{m}$ , for each composition, i.e. whatever the structure of the powder (single or multiphased materials).

Fig. 2. SEM micrographs of CCT-based powders calcined at 900 °C for 10 h. CCT-A (monophased) (a), CCT-B (biphased) (b) and CCT-C1 (three-phased) (c).



### 3.2. Ceramics

The green ceramics were sintered at 1050 °C for 24 h in static air atmosphere. The phase composition and the density of the sintered ceramics are reported in [Table 2](#). The density of the ceramics is in the range 4.5–4.8, whatever the composition. The phase composition of the ceramics is similar to the one of the powders. However, CCT-A ceramic, contrary to CCT-A powder, is a pure  $\text{CaCu}_3\text{Ti}_4\text{O}_{12}$ . No impurity of  $\text{CaTiO}_3$  is observed. For one ceramic of the CCT-C series (CCT-C3), X-ray diffraction analysis ([Fig. 3](#)) shows the presence of additional copper oxide,  $\text{Cu}_2\text{O}$  (JCPDS 78-2076). The crystallization of the  $\text{Cu}_2\text{O}$  phase, indicating the



presence of  $\text{Cu}^+$  cations, is not surprising. In fact, the  $\text{Cu}^{2+}$  cations are reduced at high temperature ( $T \approx 1000$  °C) into  $\text{Cu}^+$ . When the cooling rate is low enough, the copper cations reoxidize again during the cooling. In the present work, all the ceramics have been cooled at the same rate, i.e. 150 °C/h. In fact, the  $\text{Cu}_2\text{O}$  phase precipitates in the ceramic whose composition is the richest in copper (CCT-C3).

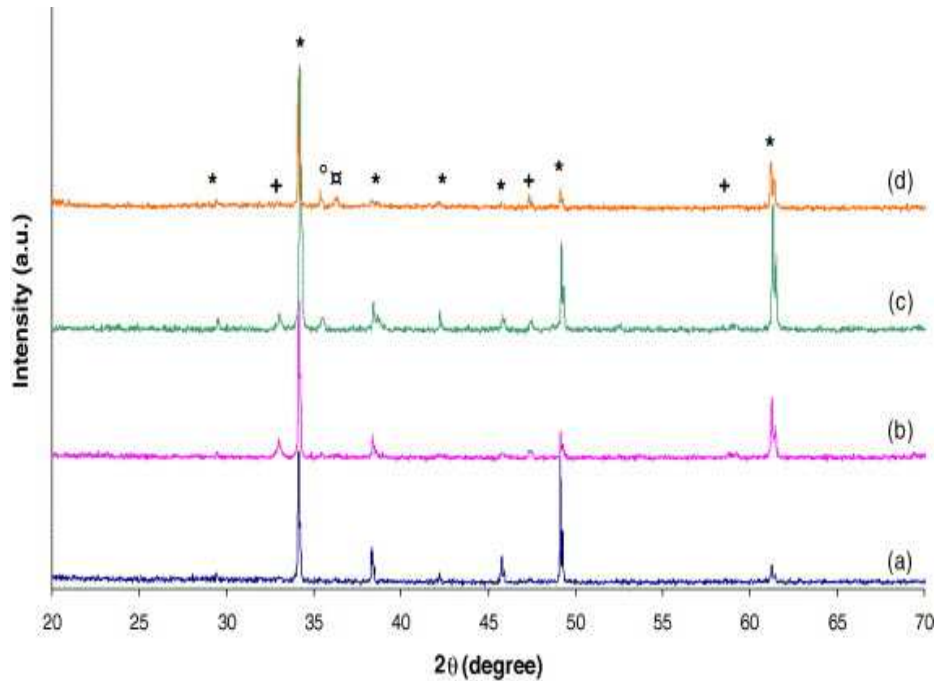
Table 2.

Density, phase composition and grain size of the CCT ceramics sintered at 1050 °C during 24 h in air

Reference	Density	Phase composition	Grain size <sup>a</sup> (μm)
CCT-A (monophased)	4.8	CCT	0.7–1
CCT-B (biphased)	4.6	CCT + $\text{CaTiO}_3$	1.5–3
CCT-C1 (3 phased)	4.8	CCT + $\text{CaTiO}_3$ + $\text{CuO}$	1–50
CCT-C2 (3 phased)	4.5	CCT + $\text{CaTiO}_3$ + $\text{CuO}$	15–90
CCT-C3 (3 phased)	4.6	CCT + $\text{CaTiO}_3$ + $\text{CuO}$ + $\text{Cu}_2\text{O}$	10–100

<sup>a</sup> Estimated from SEM observations.

Fig. 3. X-ray diffraction pattern of CCT-based ceramics sintered at 1050 °C for 24 h. monophased CCT:  $\text{Ca}_{0.25}\text{Cu}_{0.75}\text{Ti}_1\text{O}_3$  (a), biphased CCT:  $\text{Ca}_{0.25}\text{Cu}_{0.75}\text{Ti}_1\text{O}_3$  +  $\text{CaTiO}_3$  (b), three-phased CCT-C1  $\text{Ca}_{0.25}\text{Cu}_{0.75}\text{Ti}_1\text{O}_3$  +  $\text{CaTiO}_3$  +  $\text{CuO}$  (c), and CCT-C3:  $\text{Ca}_{0.25}\text{Cu}_{0.75}\text{Ti}_1\text{O}_3$  +  $\text{CaTiO}_3$  +  $\text{CuO}$  +  $\text{Cu}_2\text{O}$  (d).



The ceramic surfaces exhibit different aspects (Fig. 4). The grain sizes, determined from SEM observations are reported in Table 2. A significant difference in grain sizes is observed, ranging from approximately 1  $\mu\text{m}$  for CCT-A to a maximum of 100  $\mu\text{m}$  for CCT-C3. In fact, the huge grains are observed only in the ceramics containing the copper oxide phase (either CuO or Cu<sub>2</sub>O) (see for example the microstructure of one of the CCT-C series on Fig. 4). Moreover, those ceramics also show a particular microstructure. On the grain boundaries, a liquid phase wets the grains. In order to evidence this phenomenon, a three-phased ceramic (CCT-C1) has been quenched in air after sintering, so as to retain—at ambient temperature the high temperature microstructure. The SEM observations (in chemical contrast) of the so obtained ceramic (Fig. 5) clearly show an ex-liquid phase surrounding the CCT grains. We suspect that the copper oxide transforms into a liquid phase during the sintering treatment and leads to anomalous grain growth, as it has been reported for BaTiO<sub>3</sub>.<sup>20</sup> The ceramics containing only the CCT phase or CCT + CaTiO<sub>3</sub> have grains whose size ranges from 1 to 3  $\mu\text{m}$ , with a narrow size distribution (CCT-A and CCT-B) (Fig. 4a and b).

Fig. 4. SEM micrographs of the surface of sintered CCT-based ceramics sintered at 1050 °C for 24 h. CCT-A (monophased) (a), CCT-B (biphased) (b), three-phased CCT (C1 and C2) (c) and CCT-C3 (containing Cu<sub>2</sub>O) (d).

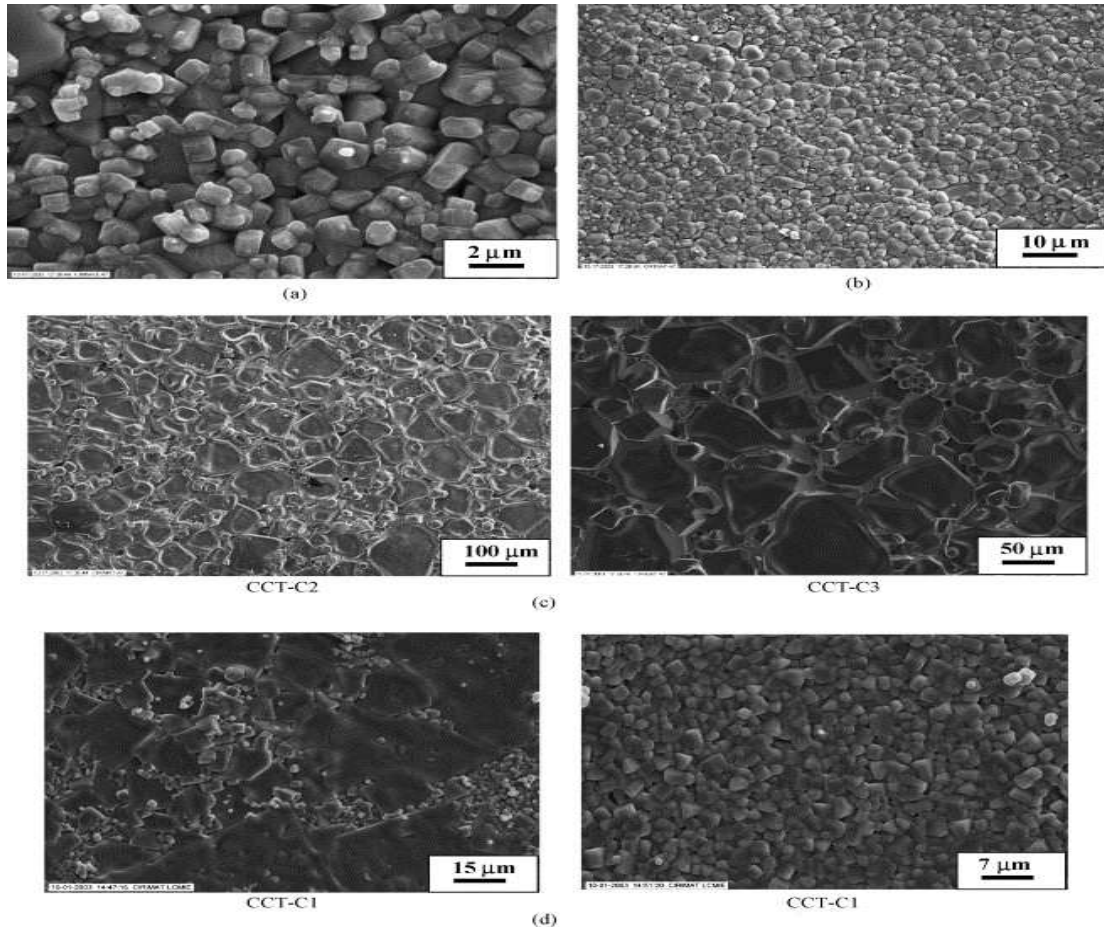
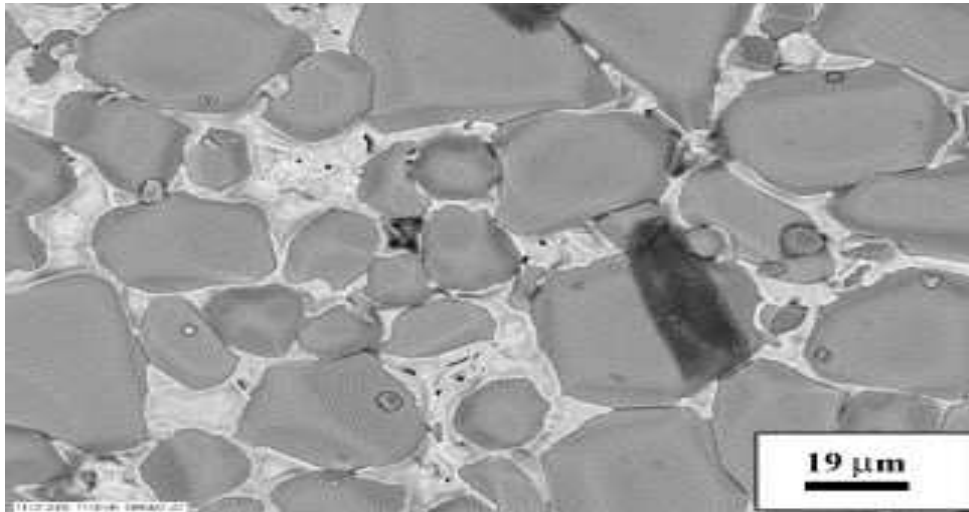
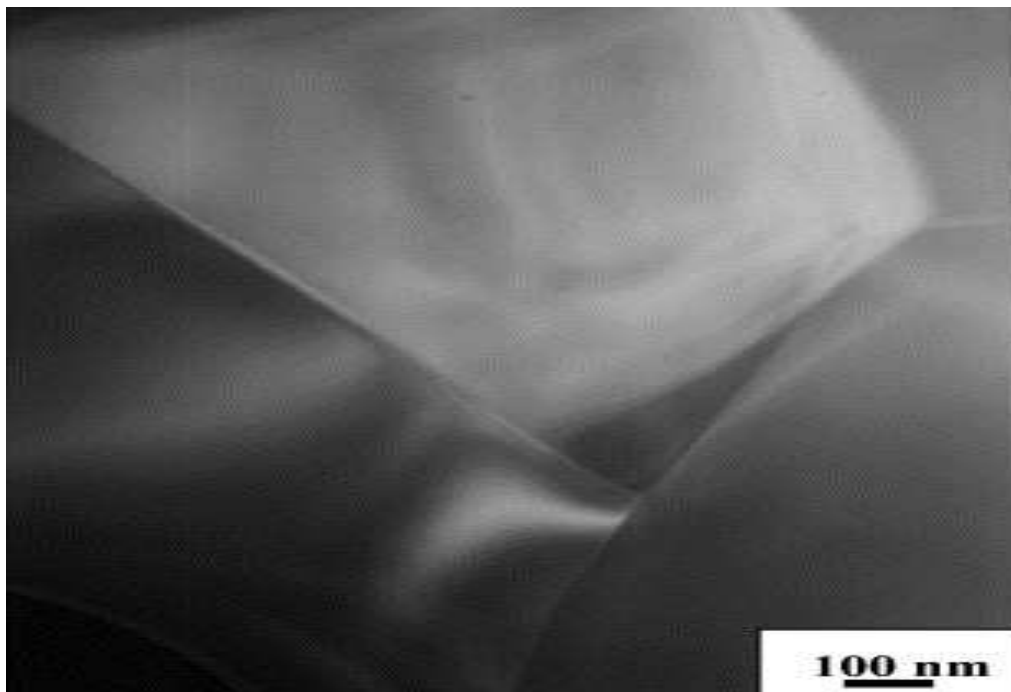


Fig. 5. SEM micrograph (chemical contrast) of the surface of a sintered CCT-based ceramics (CCT-C1) sintered at 1050 °C for 24 h and quenched in air.



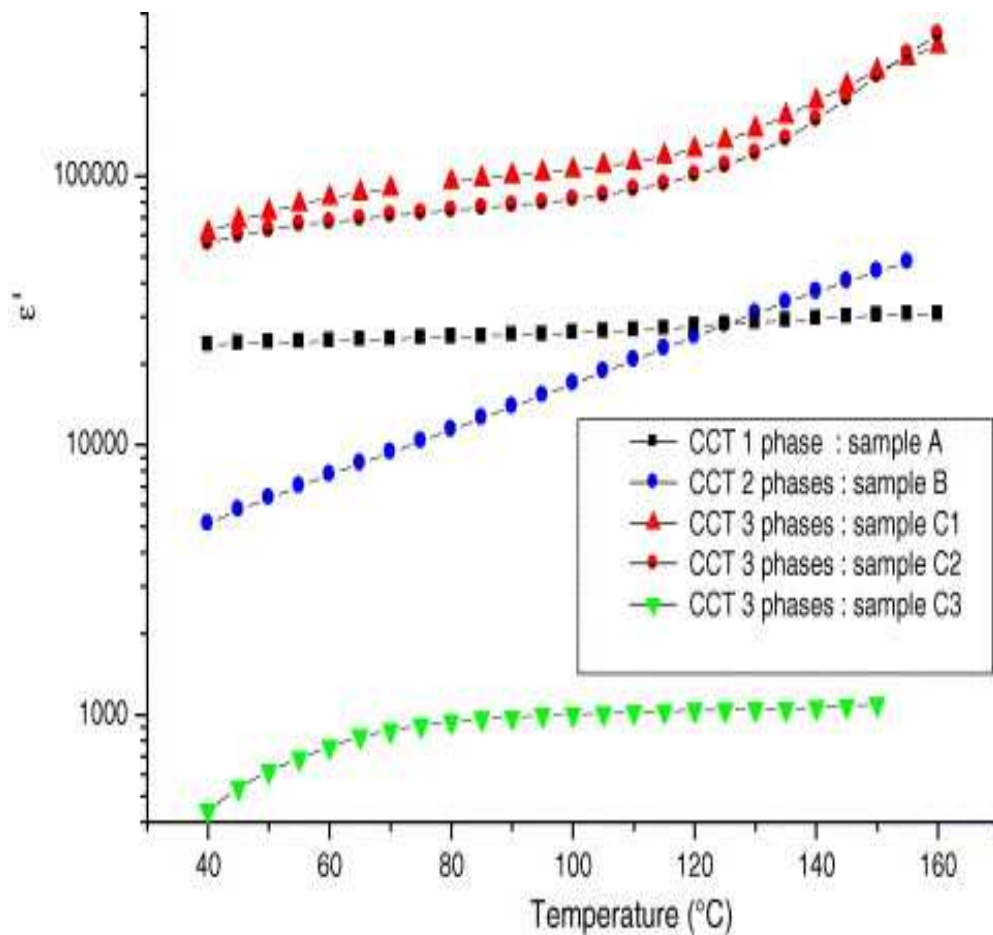
TEM observations allow detailing the structure of grain boundaries of a three-phased CCT (CCT-C1; [Fig. 6](#)). No defect is observed on the grain boundary: no particular microstructure, no twins or two-dimensional defect.

Fig. 6. TEM observations of grain boundaries of three-phased CCT (CCT-C1) ceramic sintered at 1050 °C for 24 h.



A summary of the changes in the relative permittivity, measured at 1 kHz, versus the temperature ( $40 \leq T \leq 160$  °C), is given in Fig. 7 for the different types of materials. Four different behaviors are observed. They are likely to depend on various characteristics like the ceramic structure (monophased or multiphased) and/or microstructure (grain size) and/or processing conditions.

Fig. 7. Changes in the relative part of the permittivity ( $\epsilon'$ ) ( $f = 1$  kHz) vs. temperature (range  $40 \leq T \leq 160$  °C) for the different samples.



First of all and in the temperature range under study, very high permittivity values are measured (ranging from few thousands (CCT three phases samples C3) to values higher than hundreds of thousands (CCT three phased samples C1&C2)). No ferroelectric-like transition is noticed. Moreover, a quasi-independent behavior of the permittivity with temperature is observed.

As expected the monophased CCT ceramics present the behavior already reported in the literature.<sup>1, 2, 9 and 13</sup> In this case, the permittivity is slightly higher than 20,000 and does not depend on the temperature. Biphased CCT ceramics present a linear increase of the permittivity which reaches a value of 20,000 at 120 °C. For temperature higher than 120 °C the permittivity is larger than the value obtained for monophased CCT. Last, two different behaviors are observed for the three-phased CCT materials. For the first type, permittivity values greater than  $10^5$  are observed. This value is one order of magnitude larger than the value of a monophased CCT material. This result is reproducible as it is shown for samples C1 and C2. The changes in the permittivity values of these materials are slightly temperature dependent. For the second type of materials (sample C3) the permittivity value is lower or equal to  $10^3$ , with a slight increase in the temperature range 40–60 °C. It is one order of magnitude lower than the value of a monophased CCT material.

The frequency and the temperature range of the measurement have been extended for the monophased and the three-phased materials.

Fig. 8 represents the change in the real part of the permittivity ( $\epsilon'$ ) versus the temperature at 1 kHz for the monophased and three-phased CCT. Fig. 9 gives the change in  $\text{tg}\delta$  (i.e. the dielectric losses ( $\epsilon''/\epsilon'$ )) at the same frequency (the inlet is a focus in the lowest temperature range, showing a relaxation like phenomena). It is important to notice that for temperature values up to 120–150 °C, the losses are lower than 1. For higher temperatures, the losses become so large that the capacitive nature of the material is questionable.

Fig. 8. Changes in the relative part of the permittivity ( $\epsilon'$ ) ( $f = 1$  kHz) vs. temperature (range  $-120 \leq T \leq 220$  °C) for CCT-A (monophased) and CCT-C1 (three-phased) samples.

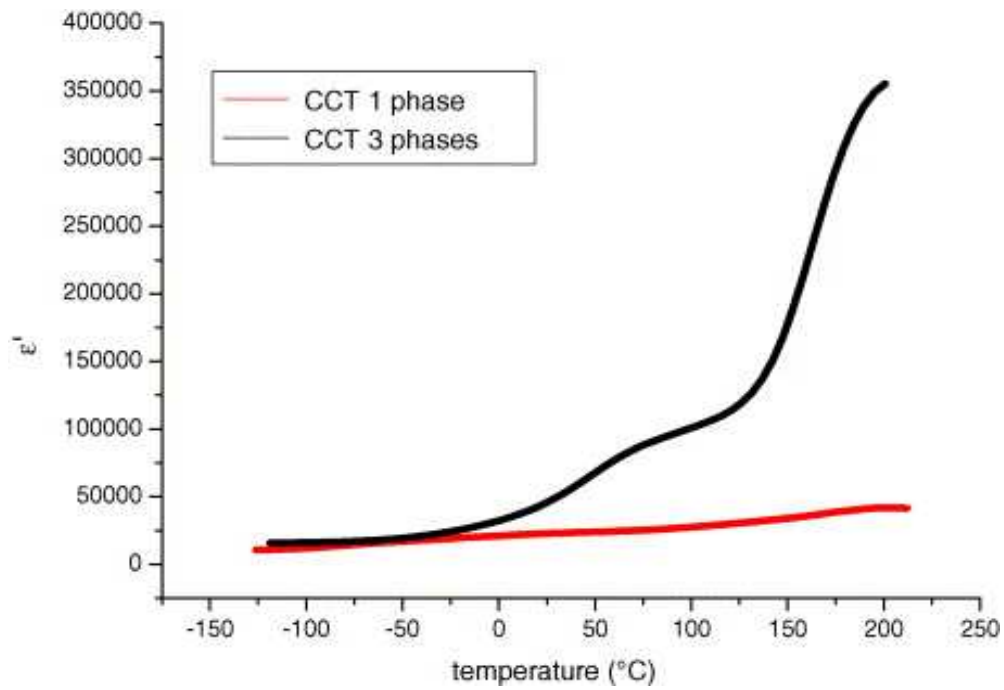
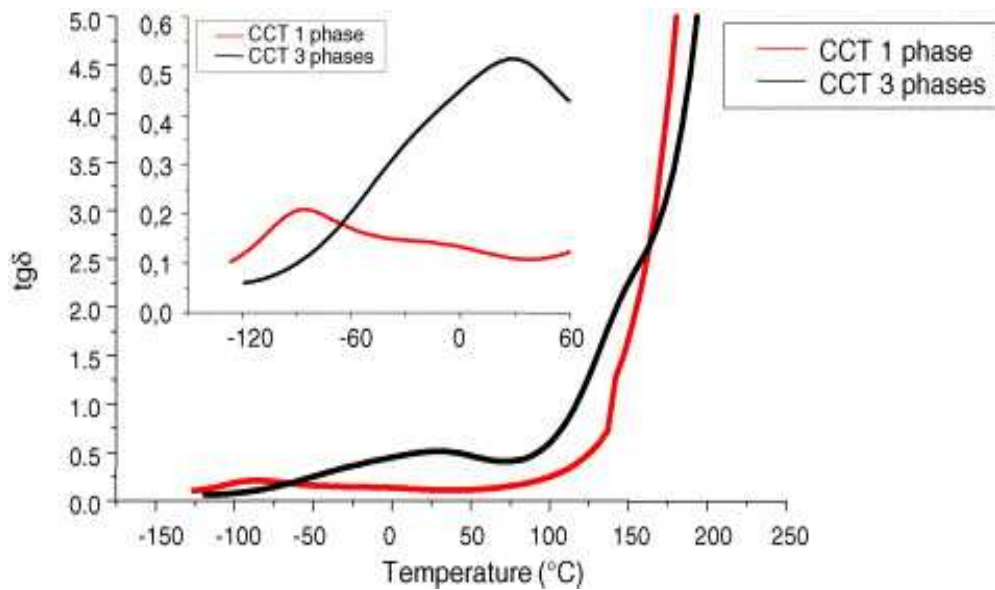


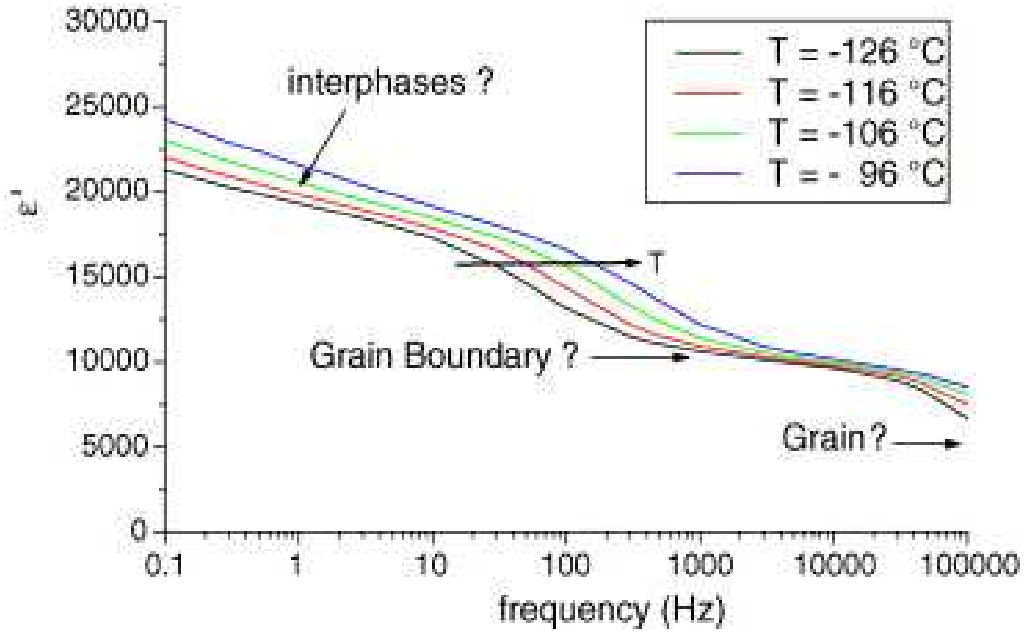
Fig. 9. Changes in  $\text{tg}\delta$  ( $f = 1$  kHz) vs. temperature (range  $-120 \leq T \leq 220$  °C) for CCT-A (monophased) and CCT-C1 (three-phased) samples.



Regarding  $\epsilon'$ , the ceramics under study do not exactly present the often reported behavior. The mechanism consists in a switch from the response of the grain boundary (which is a dielectric) to the response of the bulk regions of the material, the grains being considered as semi conductive.<sup>4</sup> This switch, always associated to a relaxation phenomenon, produces a change of at least three decades in the permittivity value. In our case and whatever the material, the permittivity does not tend to the very low value (of few tens or one hundred) reported for the lowest temperatures. The decrease in the permittivity of a CCT monophased sample is plotted in Fig. 10 at four different temperatures ( $-126\text{ }^\circ\text{C}$ ,  $-116\text{ }^\circ\text{C}$ ,  $-106\text{ }^\circ\text{C}$ ,  $-96\text{ }^\circ\text{C}$ ). It is obvious that the data show a slight increase over most of the frequency range tending to at least two different plateau, the first one in the low frequency range ( $f < 1\text{ Hz}$ ) with  $\epsilon'$  near 20,000, the second one in the intermediate frequency range ( $1\text{ Hz} < f < 10\text{ kHz}$ ) with  $\epsilon'$  near 10,000. Then a drastic drop is observed in the MHz range. With increasing the temperature, the magnitude of the permittivity increases and the different observed switches shift to higher frequencies. The two last phenomena (the plateau around 10,000 and the switch to lower values in the high frequency range) are consistent with those previously reported.<sup>1, 2</sup> and <sup>3</sup> They are attributed to the change of the physical nature of the contribution from the grain boundary to the grain as depicted in Fig. 10. Last, the existence of a first plateau for the lowest frequencies is explained by the nature of the interphases. These results will be discussed in details in the following.



Fig. 10. Changes in the relative part of the permittivity ( $\epsilon'$ ) vs. frequency, at four temperatures ( $-126\text{ }^{\circ}\text{C}$ ,  $-116\text{ }^{\circ}\text{C}$ ,  $-106\text{ }^{\circ}\text{C}$ ,  $-96\text{ }^{\circ}\text{C}$ ) for CCT-A (monophased) sample.



The changes of  $\epsilon'$  and  $\text{tg}\delta$  versus frequency are plotted at different temperatures (Fig. 11a–f and Fig. 12a–f, respectively) for the monophased and the three-phased CCT. The sudden change of  $\text{tg}\delta$  appears at various temperatures, depending on the nature of the material. All these plots demonstrate the existence of a thermally activated Debye-like relaxation in the low temperature region at an intermediate frequency which is generally attributed to a grain boundary response. Assuming an Arrhenius behavior, an activation energy may be determined according to Eq. (1):

$$f_m = \frac{1}{\tau_m} = f_{m0} \exp(-E_a/k_B T) \quad (1)$$

where  $f_m$  is the frequency of the maximum,  $E_a$  the activation energy,  $k_B$  the Boltzman constant,

Fig. 11. Changes in the relative part of the permittivity ( $\epsilon'$ ) and in  $\text{tg}\delta$  vs. frequency, at four temperatures,  $-126^\circ\text{C}$  (a),  $-96^\circ\text{C}$  (b),  $-61^\circ\text{C}$  (c), RT (d),  $57^\circ\text{C}$  (e),  $157^\circ\text{C}$  (f) for CCT-A (monophased) sample.

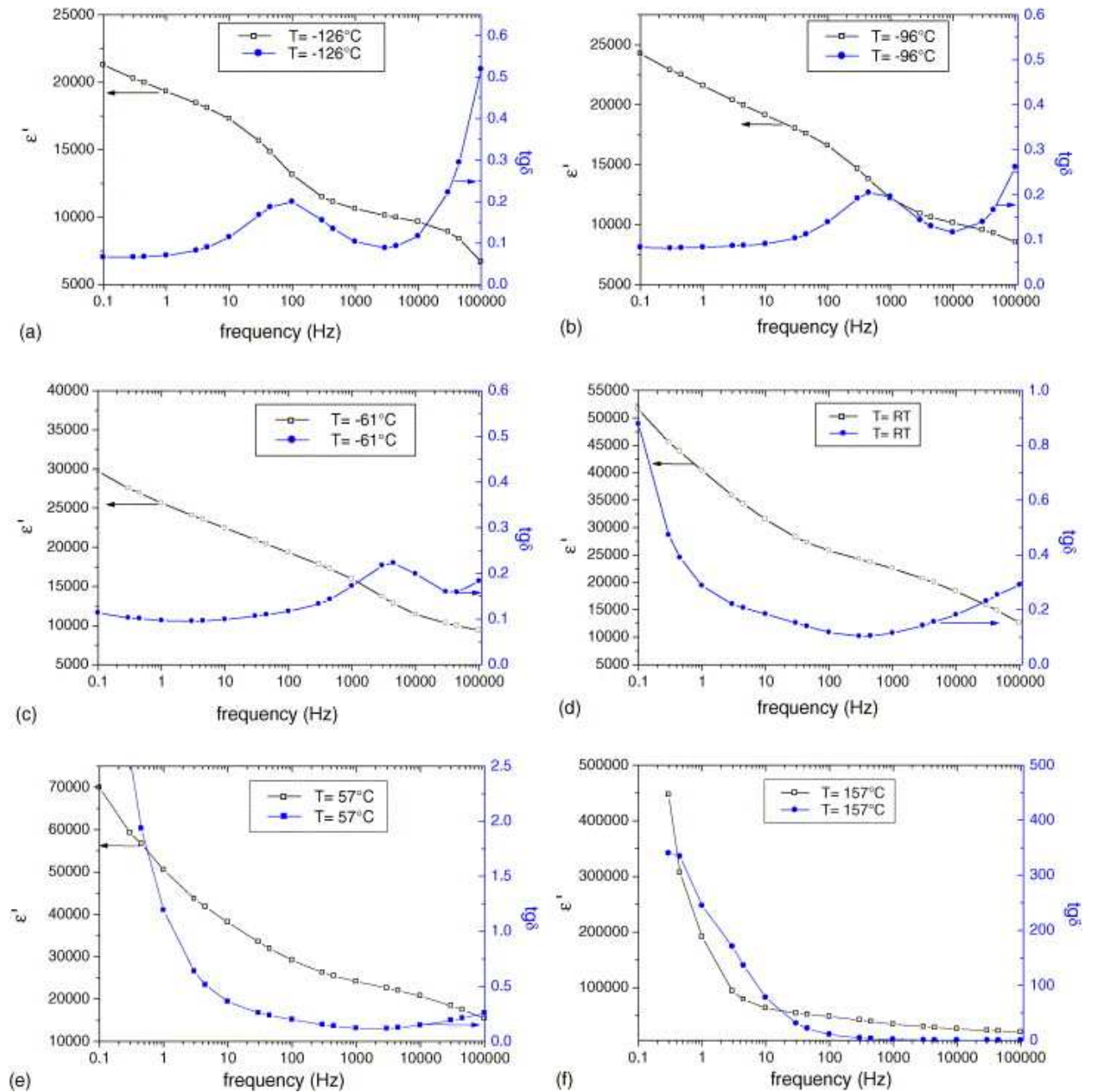
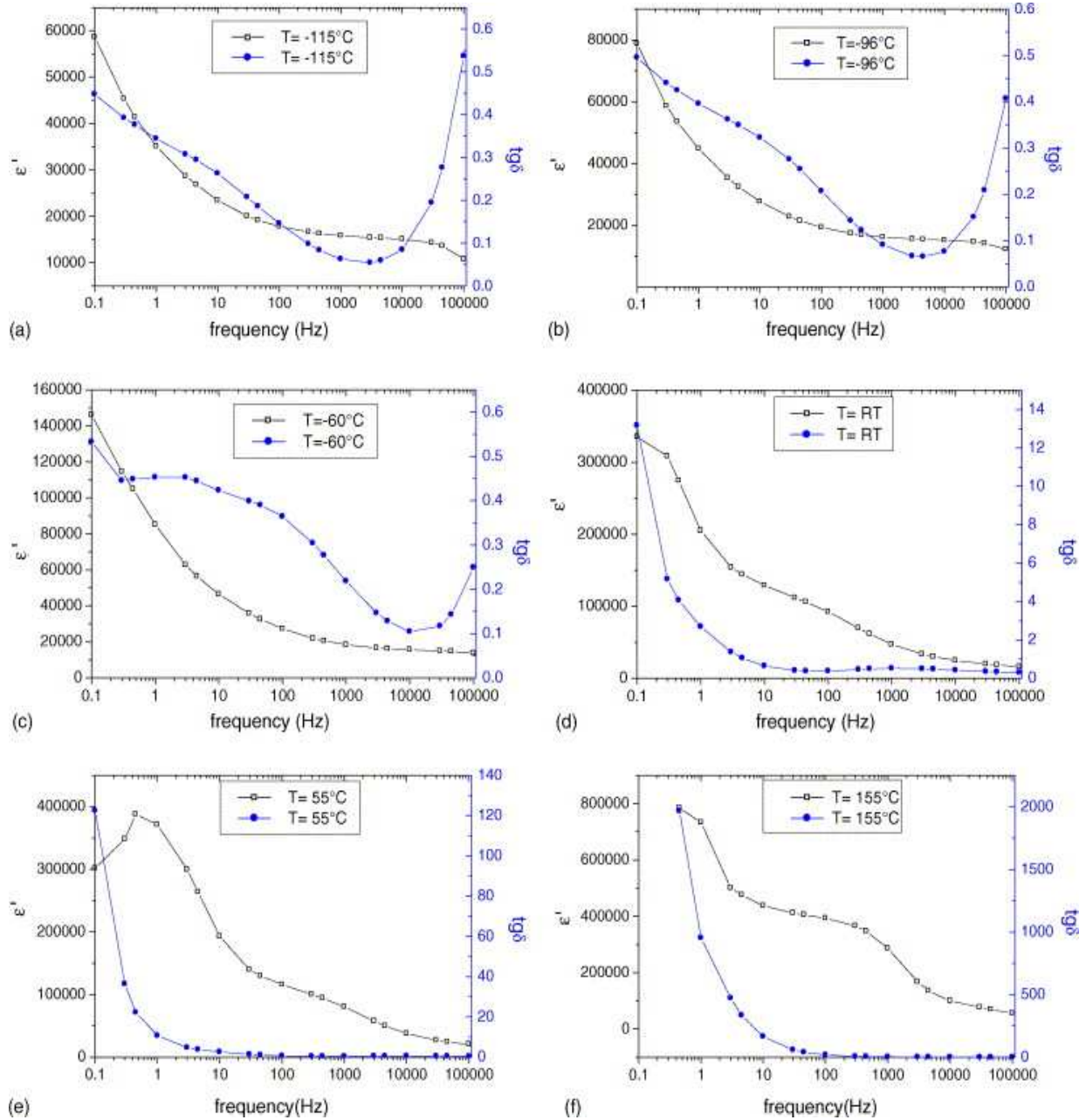


Fig. 12. Changes in the relative part of the permittivity ( $\epsilon'$ ) and in  $\text{tg}\delta$  vs. frequency, at four temperatures,  $-115\text{ }^\circ\text{C}$  (a),  $-96\text{ }^\circ\text{C}$  (b),  $-60\text{ }^\circ\text{C}$  (c), RT (d),  $55\text{ }^\circ\text{C}$  (e),  $155\text{ }^\circ\text{C}$  (f) for CCT-C1 (three-phased) sample.



A value of 0.18 eV is obtained for the monophased CCT ceramic and of 0.53 eV for the three-phased CCT materials. Regarding this last one, it is in good agreement with the one proposed by West et al.<sup>13</sup> (0.6 eV) or by Capsoni et al.<sup>29</sup> (0.54–0.73 eV) in their works on pure  $\text{CaCu}_3\text{Ti}_4\text{O}_{12}$  ceramics. The value of the activation energy for the monophased CCT sample is

quite different, ranging between the grain barrier one (near 0.6 eV) and the bulk one (0.09 eV), according to the values determined by these authors.

In summary and, whatever the material under study, (mono, bi or three-phased CCT):

- The global “classical” behavior of CCT samples is observed,
- The lowest value of the permittivity measured is at least one order of magnitude larger than the value reported in the literature. However, as illustrated in [Fig. 10](#), another drop (associated to a relaxation phenomena) is probably occurring in a frequency range higher than 1 MHz at the lowest measurement temperature (–126 °C in this case). This drop probably leads to another plateau in the permittivity value which could be measured at very low temperature (in the 10–100 K range). This temperature range is unfortunately not available in our laboratory.
- A very high value (near 400,000) is obtained for the three phases CCT at 200 °C. At this temperature, the capacitive nature of the material is questionable since the dielectric losses are very high. However, if we still consider it as a dielectric ceramic, the temperature at which this value is obtained is much lower than the one reported by Subramanian<sup>1</sup> (400 °C) to reach the same order of magnitude. Note that in<sup>1</sup> no indication of the losses is given.

Therefore, the materials under study have properties which seem to depend on their structure (nature of the different phases). These results and their most likelihood origins are discussed in the following.

## **4. Discussion**

It is obvious that, whatever the material considered (CCT-A, B or C), its electrical behavior is in marked contrast with the ferroelectric one resulting from structural distortion since no structural phase transition is detected. Therefore, this cannot be invoked to explain the electrical properties.

The three kinds of materials essentially differ from the overall chemical composition ([Table 1](#)), leading both to different grain sizes ([Table 2](#)), and particularly to different structures (monophased CCT or multiphased materials). The copper oxide phase plays an important role in these multiphased ceramics, both from the microstructural properties (grain size) and from the electrical properties. As a matter of fact, CuO has been used as an additive to lower the

sintering temperature, for example in  $(\text{Ba}_{0.8}\text{Sr}_{0.2})(\text{Ti}_{0.9}\text{Zr}_{0.1})\text{O}_3$ <sup>21</sup> material which is used as a surface barrier layer capacitor. Its melting during the sintering enhances the grain growth. In these materials, a bimodal grain size distribution with fine grained matrix containing grains exhibiting an exaggerated growth was observed. On the other hand, the amount of CuO in the ceramic seems to play an important role. Hence, for BSTZ materials, 0.5 wt.% is insufficient to improve the dielectric characteristics while more than 1 wt.% is deleterious.<sup>21</sup> In our case, an amount of more than 1 or 2 wt.% of CuO is present in the ceramics. Moreover, the huge grains observed for the ceramics containing the copper oxide (CCT three-phased series) are also probably related to the appearance of a liquid phase that “wets” the grains during the sintering.

Therefore, the role played by the grain size (strongly related to the previous discussion) has to be emphasized too. The largest the grain size (three-phased CCT) the highest the permittivity value. Hence, the monophased CCT sample presenting a sharp size distribution of small grains has the lowest permittivity. The biphased CCT sample (CCT-B) has an “in between” behavior since its permittivity value increases linearly with temperature. The permittivity is lower than the one of monophased CCT for  $T < 120$  °C and then becomes higher as the temperature increases. Last, the largest permittivity values are obtained for the three-phased ceramics (CCT-C1, and C2), i.e. the ones presenting the largest grain size. Such a behavior has already been reported in  $\text{La}_{1.5}\text{Sr}_{0.5}\text{NiO}_4$  phase<sup>22</sup> or in CCT<sup>23 and 24</sup>. It leads to the same conclusions, i.e. an increase in the grain size involves an increase in permittivity.

Finally, the particular high frequency behavior (i.e. the drop and the plateau to the low permittivity value) usually mentioned in the literature for “pure” CCT samples, is not observed in our monophased samples, even at the lowest temperature investigated. The low value of the permittivity observed once the drop has occurred is associated to the bulk (i.e. the grain itself). It is consistent with the behavior observed in other semiconducting perovskite. On the other hand, it is well known that the relaxation frequency depends on the size of the relaxing species. Our results tend to prove that the grain size of monophased CCT materials synthesized using coprecipitation is probably lower than any other CCT material reported in the literature. Another hypothesis to explain the difference observed is that the internal structure of the grain itself may be different in our case. However, the sole grain size variation cannot account for the permittivity value nor for its dependence on the number of phases present in the material.

The most plausible explanation, even if the discussion is still open, is an extrinsic origin. It is not the intrinsic structure of the material itself which confers the properties (except for the ones which could be measured at very high frequency or at very low temperature, that are related to the grain itself).

The extrinsic explanation rests on the consideration of the interfaces. Two types of interfaces have to be considered:

- the grain boundaries leading to an internal barrier layer capacitance effect<sup>13</sup>,
- the electrode interfaces leading to electrode polarization effects.<sup>25</sup>

This last point is associated to thin depletion layers which may exist at the electrodes/bulk interfaces, due to the formation of Schottky diodes. Such behavior has been observed in  $\text{CaCu}_3\text{Ti}_4\text{O}_{12}$  or  $\text{Cu}_2\text{Ta}_4\text{O}_{12}$ . The grains being conductors or at least semi-conductors, these depletion layers lead to the “apparent” colossal value of the permittivity. For the samples under study, the results obtained on CCT-C1 and CCT-C2, whose general characteristics (grain size, chemical composition, ...) and metallization do not differ from sample CCT-C3, tend to demonstrate that, at least in our case, the electrode polarization effect is not the relevant mechanism.

The high “apparent” permittivity is therefore probably associated with an internal barrier layer capacitor: the bulk of the grains would behave like other semiconducting perovskites while the grain boundaries and/or the shell would be insulating layers. Hence, for the same sample thickness, the grain size and the nature of the grain boundary are likely to have an impact on the final electrical properties. Decreasing the number of grain boundaries (by increasing the grain size) and keeping the other parameters constant, would produce an increase in the apparent permittivity, according to relation 2:

$$\varepsilon = \varepsilon_b \frac{d}{t} \quad (2)$$

where  $d$  is the grain size,  $t$  the boundary layer thickness and  $\varepsilon_b$  the permittivity of the insulating layer.<sup>25 and 26</sup>

For the biphased CCT samples, the existence of  $\text{CaTiO}_3$  (a low loss dielectric ceramic of permittivity 170<sup>27 and 28</sup>) could be considered as responsible at the same time of an increase in

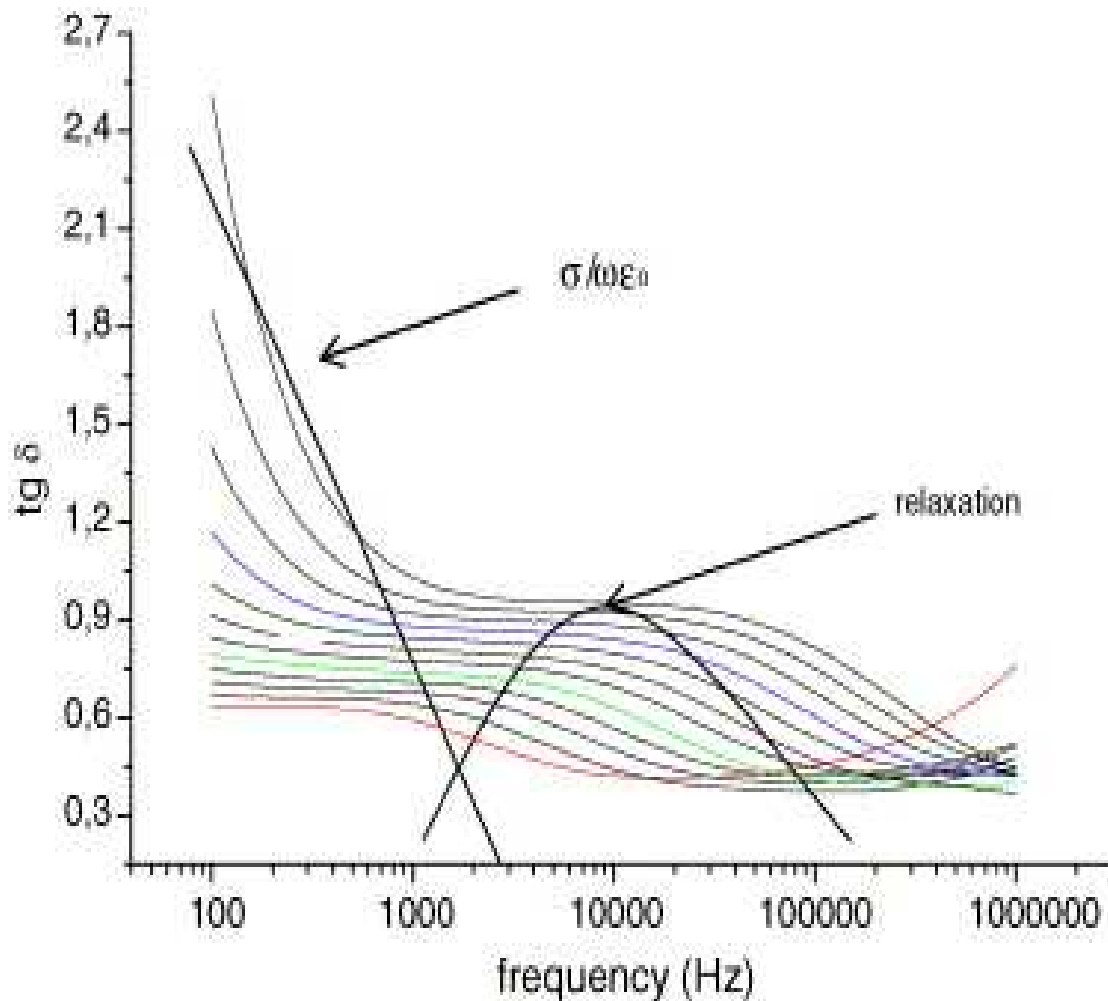
the value of the insulating layer permittivity and of a modification of the conductivity of the grains. Such an assumption could explain both the linear behavior observed and the changes in the  $\text{tg}\delta$  versus frequency. The theoretical expression of the losses ( $\text{tg}\delta$ ) is reminded:

$$\text{tg}\delta = \frac{\varepsilon''}{\varepsilon'} = \frac{(\varepsilon_r'' + \sigma/\omega\varepsilon_0)}{\varepsilon'} \quad (3)$$

where  $\varepsilon_r''$  corresponds to the part of the losses associated to the relaxation phenomena and  $\sigma/\omega\varepsilon_0$  the part due to a pure conduction mechanism, with  $\sigma$  the conductivity,  $\omega$  the pulsation and  $\varepsilon_0$  the vacuum permittivity.

In Fig. 13, the plot of  $\text{tg}\delta$  versus the frequency for different temperatures and the associated sketch makes clearly appear the possible existence of the sum of these two mechanisms.

Fig. 13. Changes in  $\text{tg}\delta$  value vs. frequency for CCT-C1 (three-phased) sample and proposed sketch.



Another possible explanation is related to the interface between the grains which is modified in the case of the multiphased material. This assumption is confirmed in the case of the three-phased CCT ceramics. The grain size increases and the presence of CuO oxide seems to play the same double role as  $\text{CaTiO}_3$  (doping of the grain boundary, modifying the permittivity value), but the melting of the copper oxide phase during the sintering treatment probably favors the wetting of the shell of the grain leading to a multilayered material as suggested before. Hence, the charge carriers' concentration at the different interfaces rises with an increase in Cu amount. More charges accumulate on both sides of the boundary layers leading to a higher dielectric constant of the samples. An optimum value of the CuO content must exist.<sup>21</sup> It has been found for CCT-C1 and CCT-C2 but not for CCT-C3 sample. It is obvious that all these assumptions have to be confirmed and works are still under progress.



## **5. Conclusion**

Different powders containing several phases,  $\text{CaCu}_3\text{Ti}_4\text{O}_{12}$  (major phase),  $\text{CaTiO}_3$  and  $\text{CuO}$  have been obtained via the calcination at  $900\text{ }^\circ\text{C}$  of the oxalate precursors, synthesized by coprecipitation. The corresponding ceramics present huge relative permittivity values and relatively low losses. The presence of additional phases ( $\text{CaTiO}_3$  and copper oxides,  $\text{CuO}$  or/and  $\text{Cu}_2\text{O}$ ) gives these ceramics a behavior different from the one observed in pure CCT materials. The relative permittivity is significantly higher than the one reported up to now (both at low temperature and at  $160\text{ }^\circ\text{C}$ ).

These CCT ceramics, presenting a real part of the permittivity higher than 250,000, are considered for internal barrier layer capacitor (IBLC) applications. It is even more remarkable that these high values can be obtained from a single step-processing route, in air, at relatively low temperature. It implies that reproducible and fine tuning of the dielectric properties of this material is possible.

## **Acknowledgements**

The authors thank Ch. Calmet for performing the SEM pictures and J.J. Demai for the TEM observations.

## **References**

- M.A. Subramanian, D. Li, N. Duan, B.A. Reisner and A.W. Sleight, High dielectric constant in  $\text{ACu}_3\text{Ti}_4\text{O}_{12}$  and  $\text{ACu}_3\text{Ti}_3\text{FeO}_{12}$ , *J. Solid State Chem.* 151 (2000), pp. 323–325.
- A.P. Ramirez, M.A. Subramanian, M. Gardel, G. Blumberg, D. Li, T. Vogt and S.M. Shapiro, Giant dielectric constant response in a copper-titanate, *Solid State Commun.* 115 (2000), pp. 217–220.
- C.C. Homes, T. Vogt, S.M. Shapiro, S. Wakimoto and A.P. Ramirez, Optical response of high dielectric constant perovskite related oxide, *Science* 293 (2001), pp. 673–676.
- D.C. Sinclair, T.B. Adams, F.D. Morrison and A.R. West, One-step internal barrier layer capacitor, *Appl. Phys. Lett.* 80 (2002) (12), pp. 2153–2155.

Y.L. Zhao, G.W. Pan, Q.B. Ren, Y.G. Cao, L.X. Feng and Z.K. Jiao, High dielectric constant in  $\text{CaCu}_3\text{Ti}_4\text{O}_{12}$  thin film prepared by pulsed laser deposition, *Thin Solid Films* 445 (2003), pp. 7–13.

B. Bochu, M.N. Deschizeaux, J.C. Joubert, A. Coullomb, J. Chevanas and M. Marezio, Synthèse et caractérisation d'une série de titanates perovskites isotopes de  $\text{CaCu}_3\text{Mn}_4\text{O}_{12}$ , *J. Solid State Chem.* 29 (1979), pp. 291–298.

S.M. Moussa and B.J. Kennedy, Structural studies of the distorted perovskite  $\text{Ca}_{0.25}\text{Cu}_{0.75}\text{TiO}_3$ , *Mater. Res. Bull.* 36 (2001), pp. 2525–2529.

Kolev, N., Bontchev, R. P., Jacobson, A. J., Popov, V. N., Hadjiev, V. G., Litvinchuk, A. P. and Iliev, M. N., Raman spectroscopy of  $\text{CaCu}_3\text{Ti}_4\text{O}_{12}$ . *Phys. Rev. B* 2002, 66, 132102-1-4.

M.A. Subramanian and A.W. Sleight,  $\text{ACu}_3\text{Ti}_4\text{O}_{12}$  and  $\text{ACu}_3\text{Ru}_4\text{O}_{12}$  perovskites: high dielectric constants and valence degeneracy, *Solid State Sci.* 4 (2002), pp. 347–351.

M.H. Cohen, J.B. Neaton, L. He and D. Vanderbilt, Extrinsic models for the dielectric response of  $\text{CaCu}_3\text{Ti}_4\text{O}_{12}$ , *J. Appl. Phys.* 94 (2003) (5), pp. 3299–3305.

A. Hassini, M. Gervais, J. Coulon, V.T. Phuoc and F. Gervais, Synthesis of  $\text{Ca}_{0.25}\text{Cu}_{0.75}\text{TiO}_3$  and infrared characterization of role played by copper, *Mater. Sci. Eng.* B87 (2001), pp. 164–168.

T.A. Adams, D.C. Sinclair and A.R. West, Giant barrier layer capacitance effects in  $\text{CaCu}_3\text{Ti}_4\text{O}_{12}$  ceramics, *Adv. Mater.* 14 (2002) (18), pp. 1321–1323.

C.C. Homes, T. Vogt, S.M. Shapiro, S. Wakimoto, M.A. Subramanian and A.P. Ramirez, Charge transfer in the dielectric constant materials  $\text{CaCu}_3\text{Ti}_4\text{O}_{12}$  and  $\text{CdCu}_3\text{Ti}_4\text{O}_{12}$ , *Phys. Rev. B* 67 (2003) (092106), pp. 1–4.

P. Lunkenheimer, V. Bobnar, A.V. Pronin, A.I. Ritus, A.A. Volkov and A. Loidl, Origin of apparent colossal dielectric constants, *Phys. Rev. B* 66 (2002) (052105), pp. 1–4.

W. Kobayashi and I. Terasaki, Unusual impurity effects on the dielectric properties of  $\text{CaCu}_{3-x}\text{Mn}_x\text{Ti}_4\text{O}_{12}$ , *Physica B* 329–333 (2003), pp. 771–772.

A.F.L. Almeida, R.S. De Oliveira, J.C. Goes, J.M. Sasaki, A.G. Souza Filho, J. Mendes Filho and A.S.B. Sombra, Structural properties of  $\text{CaCu}_3\text{Ti}_4\text{O}_{12}$  obtained by mechanical alloying, *Mater. Sci. Eng. B* 96 (2002), pp. 275–283.

P. Jha, P. Arora and A.K. Ganguli, Polymeric citrate precursor route to the synthesis of the high dielectric constant oxide  $\text{CaCu}_3\text{Ti}_4\text{O}_{12}$ , *Mater. Lett.* 57 (2003), pp. 2443–2446.

A. Douy and P. Odier, The polyacrylamide gel: a novel route to ceramic and glassy oxide powders, *Mater. Res. Bull.* 24 (1989), pp. 1119–1126.

C. Villette, Ph. Tailhades and A. Rousset, Sur l'élaboration par chimie douce de ferrites de cuivre à forts champs coercitifs, *C.R. Acad. Sci. Paris* 316 (1993) (II), pp. 1717–1723.

M. Demartin, C. Hérard, C. Carry and J. Lemaître, Dedensification and anomalous grain growth during sintering of undoped barium titanate, *J. Am. Ceram. Soc.* 80 (1997) (5), pp. 1079–1084.

C.F. Yang, Improvement of the sintering and dielectric characteristics of surface barrier layer capacitors by CuO addition, *Jpn. J. Appl. Phys.* 35 (1996), pp. 1806–1813.

Rivas, J., Rivas-Murias, B, Fondado, A., Mira, J. and Senaris-Rodriguez, M. A., Room temperature colossal dielectric constant in the charge-ordered two-dimensional nickelate  $\text{La}_{1.5}\text{Sr}_{0.5}\text{NiO}_4$  (unpublished).

A.R. West, T.B. Adams, F.D. Morrison and D.C. Sinclair, Novel high capacitance materials:  $\text{BaTiO}_3$ : La and  $\text{CaCu}_3\text{Ti}_4\text{O}_{12}$ , *J. Eur. Ceram. Soc.* 24 (2004), pp. 1439–1448.

J. Li, K. Cho, N. Wu and A. Ignatiev, Correlation between dielectric properties and sintering temperatures of polycrystalline  $\text{CaCu}_3\text{Ti}_4\text{O}_{12}$ , *IEEE Trans. Dielectrics Electr. Insulation* 11 (2004) (3), pp. 534–541.

Lunkenheimer, P., Fichtl, R., Ebbinghaus, S. G. and Loidl, A., Non-intrinsic origin of the colossal dielectric constants in  $\text{CaCu}_3\text{Ti}_4\text{O}_{12}$  (unpublished).

Wu, J., Nan, C. W., Lin, Y. and Deng Y., Giant dielectric permittivity observed in Li and Ti doped NiO. *Phys. Rev. Lett.* 2002, 89, 21, 217601-1-2176014.

K. Wakino, Recent development of dielectric resonator materials and filters in Japan, *Ferroelectrics* 91 (1989), pp. 69–86.

V.M. Ferreira, F. Azough, J.L. Baptista and R. Freer, Magnesium titanate microwave dielectric ceramics, *Ferroelectrics* 133 (1992), pp. 127–132.

D. Capsoni, M. Bini, V. Massarotti, G. Chiodelli, M. Mozzatic and C. Azzoni, Role of doping CuO segregation in improving the giant permittivity of  $\text{CaCu}_3\text{Ti}_4\text{O}_{12}$ , *J. Solid State Chem* 177 (2004), pp. 4494–4500.

Corresponding author. Tel.: +33 5 61 55 62 83; fax: +33 5 61 55 61 63.

**Original text : [Elsevier.com](http://Elsevier.com)**